

## On the cascade mechanism of short surface wave modulation

M. Charnotskii, K. Naugolnykh, L. Ostrovsky, and A. Smirnov

Zel Technologies, LLC / NOAA Environmental Technology Laboratory, 325 Broadway, Boulder, CO, 8030-3328, USA

Received: 14 July 2001 – Revised: 13 November 2001 – Accepted: 14 November 2001

**Abstract.** Modulation of short surface ripples by long surface or internal waves by a cascade mechanism is considered. At the first stage, the orbital velocity of the long wave (LW) adiabatically modulates an intermediate length nonlinear gravity wave (GW), which generates a bound (parasitic) capillary wave (CW) near its crest in a wide spatial frequency band. Due to strong dependence of the CW amplitude on that of the GW, the resulting ripple modulation by LW can be strong. Adiabatic modulation at the first stage is calculated for an arbitrarily strong LW current. The CWs are calculated based on the Longuet-Higgins theory, in the framework of a steady periodic solution, which proves to be sufficient for the cases considered. Theoretical results are compared with data from laboratory experiments. A discussion of related sea clutter data is given in the conclusion.

### 1 Introduction

Interpretation of the microwave radar and radiometric images of ocean surface structures, with scales from decameters to kilometers, entails an understanding of the modulation mechanisms of short capillary and gravity-capillary waves by long internal and surface waves. This is still a largely unclear problem and different mechanisms that contribute to this process are not well understood. For decimeter-range and longer gravity waves, adiabatic modulation by orbital velocity in still longer waves can be a main factor, e.g. Basovich and Bakhanov (1984), but for capillary ripples responsible for the scattering of centimeter- and millimeter-range radars, wind effect is typically significant. Consistent description of wind effect can be associated with modulation of air flow over the sea surface by long waves, e.g. Belcher and Hunt (1998). So far, however, at least in application to radar measurements, a typical approach has been based on the kinetic equation for

wave action with a phenomenological term describing wind effect, e.g. Hughes (1978) and Hara and Plant (1994).

In a number of cases, the aforementioned models are insufficient to adequately describe the field observations. One important piece of evidence is that a long swell with small slopes produces quite significant modulation of radar signals Ostrovsky et al. (1999). Another is the phase shift between the modulation of radar signal intensity, presumably corresponding to the ripple intensity, and Doppler signals, correlated to the orbital velocity of long waves (Hara and Plant, 1994; Kropfli et al., 1999). However, in the case of modulation by very strong internal waves, adiabatic theory may work satisfactorily even in the presence of a moderate wind (Bakhanov and Ostrovsky, 2001; Kharif, 1990).

In this relation, a “cascade” mechanism of ripple modulation seems to be of special interest. It is based on the known fact that a nonlinear gravity wave (GW) can generate “parasitic” capillary ripples (CW) near its crest in a resonant manner. Ripples propagate ahead of the crest and, due to Doppler shift produced by the orbital current in a GW, have a wide spatial frequency band. The theory of parasitic waves began with the pioneering works of Longuet-Higgins (1963) and has been further developed by different authors; (e.g. Ruvinskii and Freidman, 1981; Ruvinskii et al., 1986; Smith, 1986). The cascade, which was hypothesized, probably for the first time in Ermakov and Salashin (1994), occurs when a long wave (e.g. internal wave or swell) modulates the nonlinear GW with parasitic ripples on a GW front. Due to nonlinearity, even a moderate modulation of a GW can result in much stronger modulation of CW and, consequently, of radar and radiometric signals in corresponding frequency ranges. The idea of such a cascade is commonly accepted now but no convincing theoretical interpretation has been given so far. The damping of GW due to energy consumption by CW Ruvinskii et al. (1986) can be a possible additional mechanism of enhancing GW modulation by internal waves.

In the present paper, a consistent albeit simplified consideration of the cascade process is suggested. This consists of three stages. First, adiabatic modulation of a GW by a

long-wave current is studied. We admit an arbitrary strong modulation, including the resonant one (group synchronism). Second, analytical and mainly numerical calculations of ripples on a nonlinear GW are performed in the framework of a steady solution, based on the Longuet-Higgins (1995) theory. Although, in general, the parasitic ripples are non-stationary (see the detailed numerical work Chalikov and Sheinin, 1998), the simplified stationary theory given here seems to reflect the basic quantitative parameters of CW, as the comparison with laboratory experiments shows. Finally, we consider variations of ripples by a long wave and compare them with the data of laboratory experiments described in Ermakov and Salashin (1994).

The paper is organized as follows: Sect. 2 considers modulation of nonlinear GW by a LW; Sect. 3 discusses generation of CW by nonlinear GW; Sect. 4 presents details of numerical modelling. In Sect. 5 we compare our numerical results to laboratory data. In the conclusion we briefly discuss the relation of these results to available field data.

## 2 Adiabatic modulation of a nonlinear gravity wave

Consider first the action of the LW on the intermediate GW, producing the modulation of its amplitude and wave number by an LW current that is taken in the form of  $u(x - Ct)$ , where  $u$  is the orbital velocity in the modulating wave; suppose that  $u(x)$  is a slowly varying function of  $x$ . Such a current can be caused by a long surface or internal gravity wave that propagates in the  $x$  direction so that the problem is reduced to one-dimensional geometry. We neglect the nonlinearity of the gravity wave when calculating modulation of wave number and amplitude. Note that, even for a steepest nonlinear Stokes wave, when the wave crest curvature radius tends to zero ( $k$  is the wave number and  $H$  is crest-to-trough height), the first harmonic contains about 90% of the wave energy and the wave amplitude,  $a = H/2$ , differs from the amplitude of its first harmonic by only about 7%. After finding the modulation of a linear wave, the formulae for a nonlinear Stokes wave are used to describe variations of wave curvature and orbital velocity and finally to calculate the generated capillary waves and their modulation using the technique described below in Sect. 4. This approach can be addressed as linear modulation of nonlinear waves; it certainly cannot be used when the original GW is close to the limiting steepness and variations of the peak curvature are very sensitive to even small-amplitude variations and the higher-order terms in the dispersion equation and in the expression for wave energy should be accounted for. However, in the cases considered below, the most intensive ripple generation occurs near some “critical” wave amplitude that is not necessarily very close to the limiting amplitude, so this approach seems to be reasonably accurate. This approach is also justified by calculations of Zhang and Melville (1990) which show that, for linear LW, linear modulation theory is reasonably accurate for moderately nonlinear GW.

The linear dispersion equation for the gravity wave is:

$$\omega - (-C + u(x))k(x) = \pm\sqrt{gk(x)}, \quad (1)$$

where  $k(x)$  is a local GW wave number and  $\omega = c$  is the GW frequency in the reference frame moving with the long-wave phase velocity  $C$  where the given current is stationary. A plus sign should be used when both waves propagate in the same direction and minus in the opposite case. We neglect the effective gravity acceleration changes due to the LW here because of the small slopes and curvature associated with the LW. However, these factors are accounted for further in Eq. (11) for CW riding on much shorter and steeper GW.

The GW variations on the LW current can be found from the known equation for wave action Bretherton and Garrett (1969) or, equivalently, from the expression for average Lagrangian,  $L$ , of a surface wave Lighthill (1967). In the stationary frame considered, the period-average energy flux,  $S = \omega\partial L/\partial k$ , must be constant in  $x$ . For a linear wave this value is:

$$S = \frac{\rho\omega(\omega^2 - k^2(x)(-C + u(x))^2)}{4k^2(x)}a^2(x) = \text{const}, \quad (2)$$

where  $\rho$  is water density,  $g$  is gravity acceleration and  $a$  is the amplitude of surface displacement.

The corresponding adiabatic variations of  $k$  and  $a$  at constant  $\omega$  and  $S$  can easily be found as functions of  $u(x)$  from Eqs. (1) and (2):

$$\frac{k(x)}{k_0} = \left[ \frac{c_g + \text{sign}(C - c_g)\sqrt{c_g^2 + (C - 2c_g)(C - u(x))}}{C - u(x)} \right]^2, \quad (3)$$

where  $c_g \equiv \pm\frac{1}{2}\sqrt{\frac{g}{k_0}}$  with signs  $\pm$  corresponding to co- and counter-propagating waves, respectively.

$$\frac{a^2(x)}{a_0^2} = \sqrt{\frac{k}{k_0}} \frac{C - c_g}{C - u(x) - c_g\sqrt{\frac{k_0}{k}}}. \quad (4)$$

Here the subscript “0” refers to a point where  $u(x) = 0$ . Similar results based on the wave action conservation principle were presented in Phillips (1977).

In the examples addressed below, the LW can be considered as linear, i.e.  $u/C \ll 1$ . Therefore, one can expect that the modulation of the gravity wave is small which permits one to radically simplify these formulae. Namely, letting  $a = a_0 + \delta a$  and  $k = k_0 + \delta k$ , from Eq. (3) we obtain, for small perturbations of the wave number,

$$\frac{\delta k}{k_0} = \frac{u}{C - c_g}. \quad (5)$$

Substituting this into Eq. (4) and expanding, we have

$$\frac{\delta a}{a_0} = u \frac{3C - 4c_g}{4(C - c_g)^2}. \quad (6)$$

Evidently, the strongest modulation of both  $k$  and  $a$  occurs when the phase velocity of the long wave is close to the group velocity of the gravity wave. This is a well-known effect of group synchronism (e.g. Basovich and Talanov, 1977). Certainly, when  $|C - c_g| \sim |u|$ , modulation is not small even when  $u/C \ll 1$ , and one must use the full formulae (3) and (4).

In a particular case, when  $C \gg c_g$  (as in the case of modulation by swell or other long enough surface waves), it follows from Eqs. (5) and (6):

$$\frac{\delta k}{k_0} = \frac{u}{C}, \quad \frac{\delta a}{a_0} = \frac{3u}{4C}. \quad (7)$$

### 3 Generation of capillary waves

We describe the generation of capillary waves using the approach developed in Longuet-Higgins (1995). The pressure  $p_s(x)$  distributed over the surface of non-uniform stationary flow  $U(x)$  gives rise to a surface displacement downstream as a gravity wave and upstream as a capillary wave of the form

$$\zeta(x) = \int_x^\infty \frac{2p_s(x')F(x) \sin k^C(x' - x)}{D(x)D(x')F(x')} dx', \quad (8)$$

where

$$F(x) = \exp \left[ \int_0^x \frac{4\nu(k^C(x'))^2 U(x')}{D^2(x')} dx' \right] \quad (9)$$

is the factor presenting the effect of attenuation of the CW;

$$D(x) = (U^4(x) - 4g'(x)T)^{1/4} \quad (10)$$

describes the effect of the non-uniform flow,  $T$  is the surface tension coefficient and  $g'(x)$  is the effective gravity at the surface of the GW;

$$g'(x) = g \cos \alpha(x) - \kappa(x) U^2(x) \quad (11)$$

is related to the local surface slope  $\alpha(x)$  and centripetal acceleration;  $\kappa$  is the local surface curvature.

In our case,  $U(x)$  is the particle velocity in the GW at the free surface in a frame of reference moving with its phase speed  $C_p^G$ . Note that, in the previous section, the reference frame moved with the LW.

The local capillary wave number,  $k^C$ , is determined by the condition that the entire motion is steady in the reference frame moving with the velocity  $C_p^G$ . The corresponding dispersion relation is

$$T(k^C(x))^2 - U^2 k^C(x) + g'(x) = 0$$

and hence

$$k^C(x) = (1/2T) \left( U^2(x) + [U^4(x) - 4g'(x)T]^{1/2} \right). \quad (12)$$

Some essential features of capillary wave generation by pressure distribution  $p_s(x)$  can be seen if one considers the

behavior of Eq. (8) in the vicinity of the wave crest, where the local flow velocity and the effective gravity and viscosity can be taken as constant. For preliminary analysis we also assume that the pressure produced by the surface tension in the vicinity of the crest is modelled by a Lorentzian profile:

$$p_s(x) = T\kappa(x) = T \frac{r_{\min}}{r_{\min}^2 + 9x^2}. \quad (13)$$

Parameters of this model curvature distribution  $\kappa(x)$  are chosen in such a way that  $\kappa(x=0) = r_{\min}^{-1}$  and the angle between the tangents to the wave profile on both sides of the crest is  $120^\circ$  (i.e. the GW profile is close to a limiting one) and the crest curvature radius,  $r_{\min}$ , is much smaller than the wavelength of the GW. In this case the curvature of the crest can be estimated using asymptotic theory or direct numerical calculation of the Stokes wave profile. The approximate expression for the crest curvature radius  $r$  of the GW is, (Longuet-Higgins and Fox, 1977)

$$r_{\min} = 2.58 \frac{U_0^2}{g}. \quad (14)$$

Here  $U_0$  is the orbital velocity at the crest of the GW in the accompanying coordinate system. Note that  $r_{\min} \rightarrow 0$  for an ‘‘almost-highest’’ wave when  $U_0 \rightarrow 0$ . Substitution of Eq. (14) into Eq. (8) leads to:

$$\begin{aligned} \zeta(x) &\approx \frac{2Tr_{\min}}{D_0^2} \int_{-\infty}^\infty \frac{\sin k^C(x' - x)}{9x'^2 + r_{\min}^2} dx' \\ &= \frac{-2\pi T}{3D_0^2} \exp\left(-\frac{r_{\min} k^C}{3}\right) \sin k^C x, \end{aligned} \quad (15)$$

where

$$D_0 = (U_0^4 - U_c^4)^{1/4} \quad (16)$$

and  $U_c = (4gT)^{1/4} \approx 23.2$  cm/s is the minimal phase speed of a linear gravity-capillary wave.

Substitution of  $r_{\min}$  from Eq. (14) and the expression for  $D_0^2$  lead to the following equation for the amplitude of the CW

$$\zeta_a = \frac{2\pi T \exp\left(-\frac{5.155}{3U_c^4} U_0^2 \left[ U_0^4 + (U_0^4 - U_c^4)^{1/2} \right]\right)}{3(U_0^4 - U_c^4)^{1/2}}. \quad (17)$$

It is seen from this equation that the CW amplitude grows for steeper GW when  $U_0$  decreases to the values close to  $U_c$ . At some intensity of GW the denominator  $D_0$  in Eq. (17) tends to zero. This is the ‘‘critical regime’’ of the CW excitation, when the orbital velocity of GW prevents the CW propagation down the slope of the GW; the effect of ‘‘blocking’’ of CW takes place and its intensity increases Longuet-Higgins (1995). It should also be noted that when  $U_0$  is substantially larger than  $U_c$ , the exponent in Eq. (17) becomes extremely small. This reflects the coherent averaging of CW over a finite width of pressure distribution.

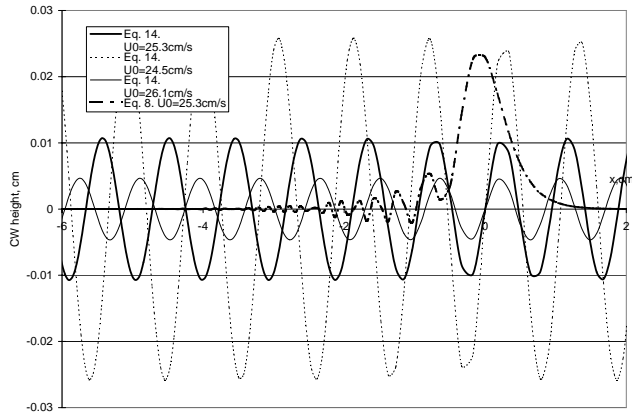


**Fig. 1.** CW profiles calculated according to a simple analytical model (15) and by direct integration of Eq. (8).

Small perturbations of GW amplitude lead to a pronounced modulation of the CW. This is illustrated by results of direct calculations according to Eq. (17) presented in Fig. 1, where we show CW profiles calculated according to Eqs. (15) and (17). Small, 3% changes of  $U_0$ , cause approximately 250% changes in CW amplitude. The direct numerical integration, according to Eq. (8) for a 30-cm-long GW with the same value of  $U_0$ , supports this result qualitatively but provides a much more complicated CW waveform. Besides overall ripple decay with distance from the GW crest,  $x = 0$ , due to viscous dissipation, one can notice substantial changes of CW wavelength not accounted for in the simple analytical model of Eqs. (15) and (17).

The stationary ripple situation considered here is simpler but also is more restricted in comparison with Chalikov and Sheinin (1998), where the nonstationary problem was solved numerically. On the other hand, it can be expected that for a limited time interval the ripples will remain synchronous with the gravity wave, especially in the presence of significant losses. Also, the present approach is linear with respect to CW, uses adiabatic modulation of CW which is valid only if  $k^C \gg k$  and does not account for dissipation of GW due to CW generation. A more complicated theory of stationary ripples, based on viscous boundary layer approximation, was proposed by Fedorov and Melville (1998) who addressed these issues and showed excellent agreement with an experiment for short GW Fedorov et al. (1998). However, for the present study of cascade modulation of CW we consider the simpler Longuet-Higgins (1995) model to be adequate. To achieve a more realistic description of CW modulation it is necessary to account for the effects of non-uniform flow, viscosity and variation of gravity acceleration. This was done numerically, and the corresponding results are presented in the next section.

#### 4 Numerical modeling

Calculation of CW generation by GW was performed by numerical integration of Eq. (8), for model nonlinear irrota-

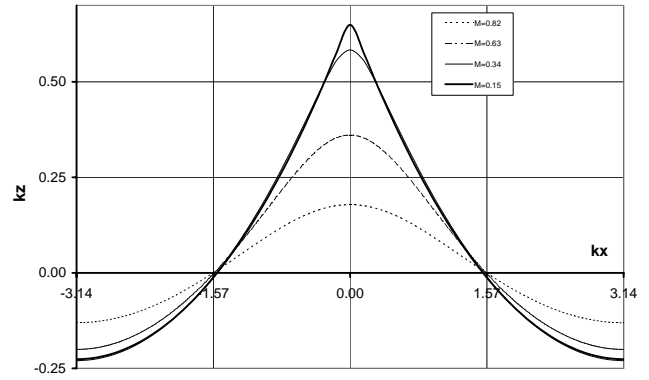


**Fig. 2.** Normalized profiles of Stokes wave of different amplitude.

tional gravity waves generated numerically, using the technique proposed in Chalikov and Sheinin (1998). This technique is based on conformal mapping and Fourier series expansion. Figure 2 presents examples of the GW profiles obtained. Parameter  $M = U_0/C_p^G$  is the dimensionless orbital velocity at the wave crest in the coordinate system moving with the GW phase speed. For the steepest possible GW,  $M = 0$  and for gentle linear waves  $M \rightarrow 1$ . The number of Fourier harmonics used in computations varied from 512 for  $M = 0.82$  to 2048 for  $M = 0.15$ . In the case of modulated GW we recalculated relevant curvature, slope and orbital velocity distributions for each  $k$  and  $a$  combination.

To verify the CW model, we have compared the results with experimental data of Chang et al. (1978). Figure 3 shows our computational data, which should be compared to Figs. 5 and 6 of Chang et al. (1978). It is seen that the calculated ripple amplitude is in a good agreement with the experiment. The major difference is that the experiment shows a stronger damping of ripples than what follows from the theory. This may be attributed to a larger effective viscosity than the molecular viscosity used in the theory and/or finite resolution of laser slope gauge. We also compared our calculations to the measured data presented in Fig. 4 of Fedorov et al. (1998). Figure 4 presents our calculation results for GW frequency  $f = 4Hz$  which are in good agreement with the data of Fig. 4c of Fedorov et al. (1998) after a slight adjustment of the wave amplitude. Our calculations for  $f = 5Hz$  and  $f = 6Hz$  produced very strong ripples that clearly violate the assumption of CW linearity. Note also that, for these frequencies, the wavelength of stationary ripples is only 8–15 times smaller than the GW wavelengths which makes adiabatic modulation of CW at the front of GW questionable. Figure 5 shows examples of ripple wave profiles generated by GW of 12 cm wavelength. For the weakest GW considered,  $M = 0.63$ , surface tension causes only small and smooth changes of the gravity wave profile and no ripples are present. This can be explained by strong averaging of short capillary waves by smooth curvature distribution as mentioned in the previous section. For  $M = 0.50$  the GW is not yet very steep (maximum slope is about 0.38) but the situation is already close to critical Longuet-Higgins (1995);

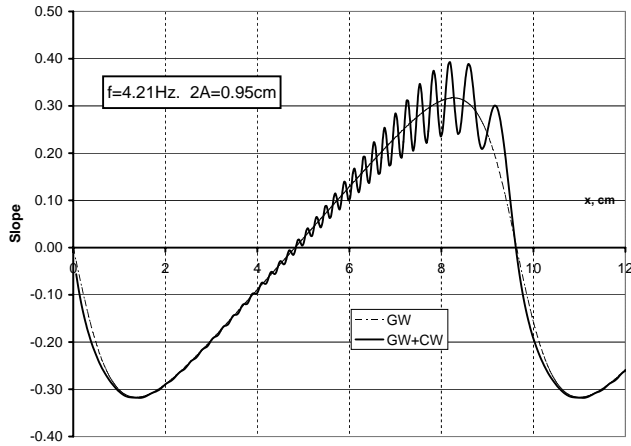


**Fig. 3.** Slope profile of GW (light solid curve) and GW with ripples (heavy solid curve) for experimental conditions of Chang et al. (1978).

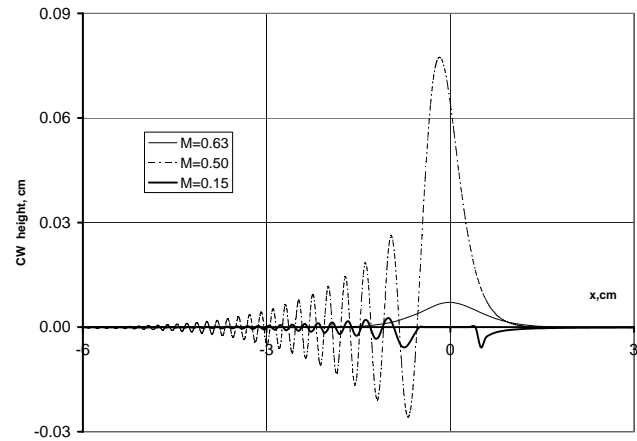


**Fig. 5.** Ripple waveforms for the 12 cm gravity waves with  $M = 0.63; 0.5; \text{ and } 0.15$ .

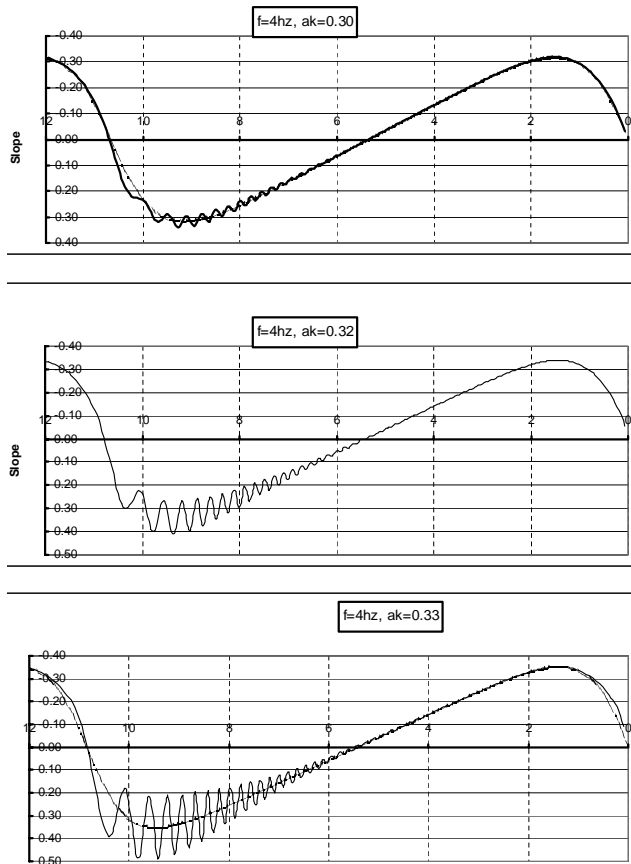


**Fig. 4.** Slope profiles of GW (light solid curve) and GW with ripples (heavy solid curve) for experimental conditions of Fedorov et al. (1998). Wave frequency  $f = 4.0\text{ Hz}$ , dimensionless wave amplitude indicated on charts.

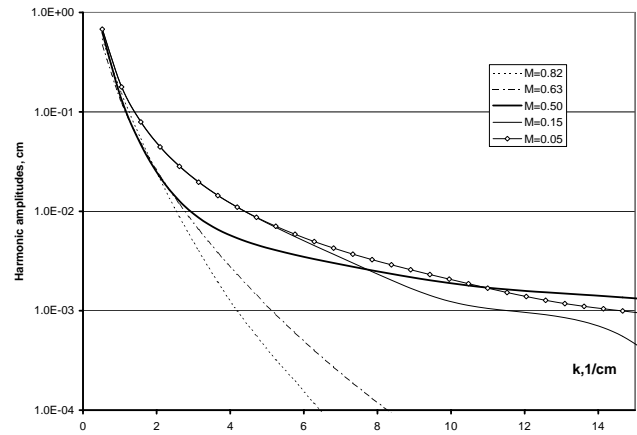


**Fig. 6.** Amplitudes of harmonics for 12 cm gravity waves of various amplitudes with ripples.

the CW is actively generated at all points of the surface of the GW. Note that for a chosen wavelength and kinematic viscosity  $\nu = 0.01\text{ cm}^2\text{ s}^{-1}$  used for all calculations, there is practically no “leakage” of ripples to adjacent periods of

GW. Further decrease to  $M = 0.15$  creates a supercritical situation for CW near the GW crest. In this case stationary ripples cannot appear near the crest, where capillary forces are strongest, which causes an overall decrease of ripple amplitude. Our modelling shows that this situation remains qualitatively similar for longer GW; a gentle wave creates no ripples, the largest ripples appear close to the critical regime and, for a supercritical case, the ripples are damped. Also, the numerical modelling confirms that a slightly modulated GW can yield a strong variation of ripples. As seen from Fig. 5, the change of  $M$  by about 25% causes ripple amplitude variation by an order of magnitude. Figure 6 shows amplitudes of harmonics for the 12-cm GW with ripples. A narrow spectrum for  $M = 0.82$  presents primarily GW in the absence of ripples. Note that the generation of ripples substantially increases the width of the spectrum. It is also interesting that the combined effects of ripple generation, averaging and supercriticality causes non-monotonous dependence of certain spectral components on the amplitude of GW. This circumstance can be important for interpretation of radar scattering discussed below.

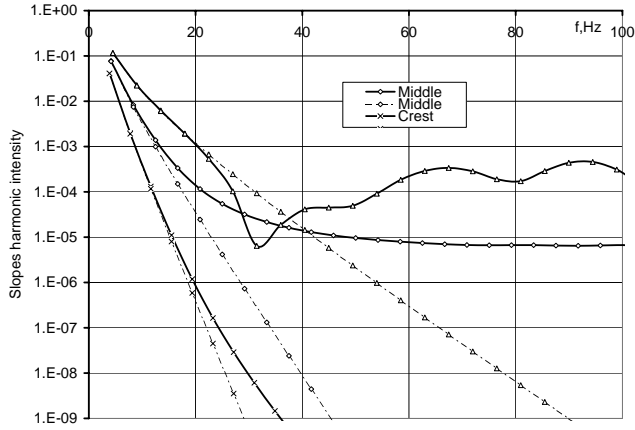


**Fig. 7.** Harmonic intensities of slopes of gravity waves (dashed-dotted line) and gravity waves with parasitic ripples (solid line) at different positions along modulating internal wave for experimental conditions of Bakhanov et al. (2000).

## 5 Comparison with experimental data

Although a relatively large body of literature already exists concerning ripple generation by internal waves, only a few controlled experimental studies of a cascade-type ripple modulation are known. These are primarily Russian works on laboratory experiments where nonlinear GW with ripples were modulated by internal waves (IW); (Ruvinskii et al., 1986; Ermakov and Salashin, 1994; Bakhanov et al., 2000). Here we compare our results with the series of experiments reported in Ermakov et al. (2000). In the experiment in question, the IW was excited in the tank with an approximately two-layer stratification, each layer of about 15 cm thickness. The density jump  $\Delta\rho$  was  $0.04 \text{ g cm}^{-3}$ , internal wave period was 9.8 s and amplitude,  $\eta$ , of pycnocline displacement was 0.2 cm and 0.4 cm in two series of measurements. The surface wave, of frequency 4 Hz, wavelength  $\lambda = 9.76 \text{ cm}$  ( $k_0 \approx 0.644 \text{ rad/cm}$ ) and amplitude in the range of several mm was generated by wavemaker. In this experiment the GW modulation by IW was measured.

Based on these data, we calculated the phase velocity  $C$  of the linear IW in a two-layer fluid:

$$C = \sqrt{\frac{g\Delta\rho}{\rho} \frac{h_1 h_2}{H}} \approx 16 \text{ cm s}^{-1}, \quad (18)$$

where  $H = h_1 + h_2$  and  $h_{1,2}$  are thicknesses of layers. From here, the IW wavelength  $\lambda_{IW} \approx 157 \text{ cm}$ . The horizontal current created by the IW at the surface, for IW amplitude 4 mm, can be found as

$$u = -C \frac{\eta}{h_1} \approx 0.46 \text{ cm s}^{-1}. \quad (19)$$

Since  $u/C \approx 3\%$ , the IW is linear and the modulation of the surface gravity wave can be assumed to be small. The GW wavelength is small in comparison with that of the IW,  $\lambda \ll \lambda_{IW}$ , so the formulae (3) and (4) obtained for slow modulation should work sufficiently well.

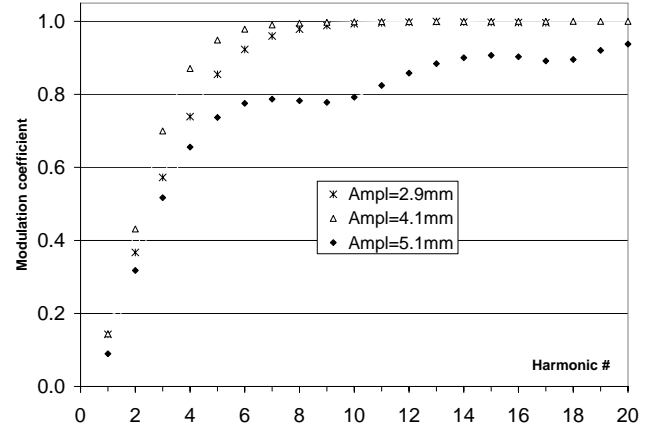


**Fig. 8.** Modulation coefficients for the first 20 harmonics for experimental conditions of Ermakov et al. (2000).

Note that the group velocity of the gravity wave,  $c_g = \frac{1}{2}\sqrt{g/k_0}$ , is about 19.5 cm/s i.e. it slightly exceeds the IW velocity. From Eq. (3),

$$\frac{\delta k}{k} \approx -0.10 \quad (20)$$

and from Eq. (4),

$$\frac{\delta a}{a_0} \approx -0.19. \quad (21)$$

Both  $\delta k$  and  $\delta a$  are in anti-phase with  $u$  and in phase with  $\eta$ . This phasing agrees with the experiment of Bakhanov et al. (2000) as well as the amplitude modulation coefficient, which is close to the measured value of 0.2. Note also that modulation coefficients for both amplitude and wave number are significantly larger than  $u/C$ . This is caused by proximity to group synchronism discussed in Sect. 2. Hence, notwithstanding that GW modulation is small, we must use more complicated formulae (3) and (4) instead of Eqs. (5) and (6). Figure 7 presents computational results for spectral intensities of surface slopes at the middle point, crest and trough of IW for these experimental conditions for the case when the unmodulated amplitude of GW is 4.5 mm. It shows substantial changes of the high-frequency part of slopes spectra, associated with ripple generation due to a cascade mechanism, as compared to a “pure” nonlinear GW; the latter spectra are shown as dashed-dotted lines. It is clear again that relatively small 10–20% changes of the GW amplitude and wave number cause orders of magnitude intensity changes for higher harmonics. At the same time, the lowest harmonics show no large changes. Note also that the shape of the computed spectrum is close to the measured spectrum presented in Fig. 27 of Bakhanov et al. (2000). Figure 8 presents modulation coefficients calculated for the first 20 harmonics of GW with ripples for a 2 mm amplitude of IW and various amplitudes of nonlinear GW. Comparison of these results with experimental data presented in Fig. 4 of Ermakov et al. (2000) shows the same principal features; a fast growth of modulation coefficient for the first 5–7 harmonics

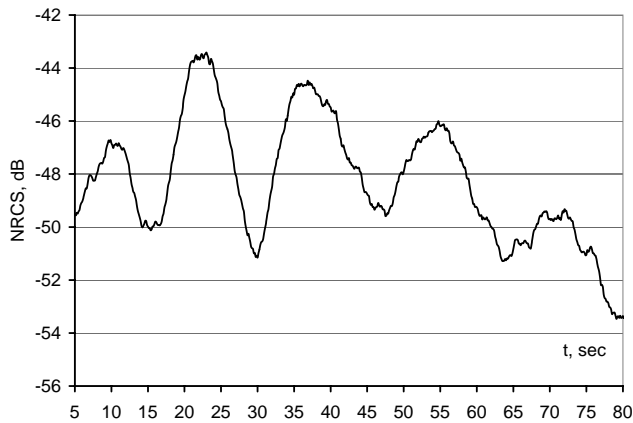


**Fig. 9.** Time series of NRCS at vertical polarization, obtained on 23 September 1995, at 01:28:00 UTC. The radar beam was fixed at azimuth  $257^\circ$  over 317 s. Winds are 4 m/s from  $212^\circ$ . Significant wave height is 2.3 m.

and saturation for higher numbers. Calculated modulation coefficients are close to those in experimental data for the first two harmonics. However, calculations predict an almost 100% modulation coefficient for higher harmonics whereas the measured values are 60–70%. This discrepancy can be related both to the accuracy of the adiabatic modulation approximation we used and to the accuracy of measurements, since data presented in Fig. 2 of Ermakov et al. (2000) show at least 80% modulation for the amplitude of the 17th harmonic. Lower modulation coefficients, for  $a = 5.1$  mm in Fig. 8, correspond to a very specific situation when ripples are strongest at the midpoint between the crest and trough of the IW. For the IW crest where GW amplitude is lowest, the generation of ripples is suppressed by coherent averaging, as shown by the exponent in Eq. (17). For the IW trough, the GW is steeper and we have a supercritical situation for most of the GW crest area; ripples are also relatively small. Other calculations show that competition of these two effects can cause a reverse modulation phase with respect to IW and doubling of modulation frequency for higher harmonics.

## 6 Discussion and conclusion

The simplified model for parasitic ripples and cascade modulation of their spectra by long waves, suggested and elaborated above, demonstrates reasonably good agreement with the data of laboratory experiments on ripple generation and modulation by internal waves. The computational results for spectral intensities of surface slopes at the middle point, crest and trough of IW, for experimental conditions in a tank, show substantial changes of the high-frequency part of these spectra associated with ripple generation due to a cascade mechanism compared to a “pure” nonlinear GW. It is demonstrated that relatively small 10–20% changes in the GW amplitude and wave number cause orders of magnitude intensity changes for higher harmonics. At the same time, the lowest harmonics show no large variation. Note also that the shape

of the computed spectrum for nominal GW amplitude, about 4.5 mm, is very close to the measured spectrum.

In a laboratory experiment by Plant et al. (1999), the GWs were excited by wind and Doppler spectra of a scattered radar signal were measured. According to the authors, parasitic capillary waves prevail over the wind-generated ripples when the wind friction velocity is smaller than 20 cm/s. For real seas, depending on the stability of the atmosphere, this may correspond to a standard wind of about 3–6 m/s. Despite a rather large body of experimental material regarding radar scattering from the sea surface, uncertainty still exists regarding the cascade mechanism contribution as opposite to the direct modulation of short wind-induced waves by long waves. One of the main difficulties here is that the intermediate GWs have a broad frequency spectrum which complicates direct application of theoretical results and laboratory data to real sea conditions.

However, even at present, the features of cascade mechanisms can provide possible interpretation of some experimental data. An example is the modulation of radar returns by swell in the Coastal Ocean Probing experiment (COPE '95), including the data reported in Kropfli et al. (1999) and Ostrovsky et al. (1999). Figure 9 shows a time series for a radar scattering cross section at vertical polarization in the presence of swell with an amplitude of about 1 m and a period of about 16.5 s. The modulation depth reaches 5 dB and the modulation period matches a period of swell. The estimates, according to Eq. (7) which is well applicable in this case, provide the adiabatic modulation coefficient for a gravity wave (same order for a capillary-gravity wave) of about 1.3%. This seems insufficient to explain the strong modulation of scattered signal shown in Fig. 9. At the same time, as shown above, the parasitic ripple amplitude and spectrum are very sensitive to even slight changes of nonlinear GW amplitude, especially near critical value (see Fig. 5), so that a cascade mechanism can readily provide 5 dB variation of ripple energy. Hence, a cascade mechanism is plausible here, especially for light winds. Also, as COPE results show, for light winds (about 0–3 m/s), modulation of intensity and Doppler signal are in phase Ostrovsky et al. (1999) which implies that the strongest variations occur at the crests of swell which corresponds to the theoretical prediction. To obtain more insight in to this problem, further processing of field data is needed. From a theoretical perspective, an important problem is to consider ripple generation and cascade effect for a broad distribution of GW crest amplitudes imitating the real sea roughness.

## References

- Bakhanov, V. V., Dolina, I. S., Ermakov, S. A., Gopalo, I. I., Kazakov, V. I., Kemarskaya, O. N., Korotkov, D. P., Konnov, I. R., Reznik, S. N., Serin, B. V., and Sergievskaya, I. A.: Laboratory modeling of interactions between waves and flows in the upper ocean, ed.: L. A. Ostrovsky NOAA Tech Memo. OAR ETL-299, 29–45, 2000.

- Bakhanov, V. V. and Ostrovsky, L. A.: The action of strong internal solitary waves on surface waves, *J. Geophys. Res.*, submitted, 2001.
- Basovich, A. Ya. and Talanov, V. I.: On the transformation of short surface waves on non-uniform currents, *Izv. AN SSSR, FAO*, 13, 766–773, 1977.
- Basovich, A. Ya. and Bakhanov, V. V.: Surface wave kinematics in the field of an internal wave, *Izvestia, Atmos. Ocean. Phys.*, 20, 50–54, 1984.
- Belcher S. E and Hunt, J. C. R.: Turbulent flow over hills and waves, *Ann. Rev. Fluid Mech.*, 30, 507–538, 1998.
- Bretherton, F. P. and Garret, C. J. R.: Wavetrains in inhomogeneous moving media, *Proc. Roy. Soc. London*, 529–554, 1969.
- Chalikov, D. and Sheinin, D.: Direct modeling of one-dimensional nonlinear potential waves, in *Nonlinear Ocean Waves*, (Ed) Perrie, W., *Advances in Fluid mechanics*, 17, 207–258, 1998.
- Chang, J. H., Wagner, R. N., and Yuen, H. C.: Measurement of high frequency capillary waves on steep gravity waves, *J. Fluid Mech.*, 86, 401–413, 1978.
- Ermakov, S. A. and Salashin, S. G.: On the effect of strong modulation of capillary-gravity ripples by Internal waves, *Doklady AN*, 337, 1, 108–111, 1994.
- Ermakov, S. A., Sergievskaya, L. A., Shchegolkov, Yu. B., and Goldblat, V. Yu.: Wave tank study of “cascade” modulation of bound capillary-gravity waves due to internal waves, *Proceedings of IEEE 2000 International Geoscience and Remote Sensing Symposium*, Honolulu, Hawaii, 1087–1089, 2000.
- Fedorov, A. V. and Melville, W. K.: Nonlinear gravity-capillary waves with forcing and dissipation, *J. Fluid Mech.*, 354, 1–42, 1998.
- Fedorov, A. V., Melville, W. K., and Rosenberg, A.: An experimental and numerical study of parasitic capillary waves, *Phys. Fluids*, 10, 1315–1323, 1998.
- Hara, T. and Plant, W.: Hydrodynamic modulation of short wind-wave spectra by long waves and its measurement using microwave backscatter, *J. Geophys. Res.*, 87, 9767–9784, 1994.
- Hughes, B. A.: The effect of internal waves on surface wind waves, *J. Geophys. Res.*, 83, 455–465, 1978.
- Kharif, C.: Some aspects of the kinematics of short waves over longer gravity waves in deep water, *NATO ASI series. Series E, Applied sciences*, 178, 265–279, 1990.
- Kropfli, R. A., Ostrovsky, L. A., Stanton, T. P., Skirta, E. A., Keane, A. N., and Irisov, V.: Relationships between internal waves in the coastal zone and their radar and radiometric signatures, *J. Geophys. Res.*, 104, 3133–3148, 1999.
- Lighthill, M. J.: A discussion on nonlinear theory of wave propagation in dispersive systems, *Proc. Roy. Soc. London*, A299, 28–53, 1967.
- Longuet-Higgins, M. S.: The generation of capillary waves by steep gravity waves, *J. Fluid. Mech.*, 16, 138–159, 1963.
- Longuet-Higgins, M. S.: Parasitic capillary waves: a direct calculation, *J. Fluid. Mech.*, 301, 79–107, 1995.
- Longuet-Higgins, M. S. and Fox, M. J. H.: Theory of the almost-highest wave: the inner solution, *J. Fluid. Mech.*, 80, 721–741, 1977.
- Longuet-Higgins, M. S. and Fox, M. J. H.: Theory of the almost-highest wave. Part 2 Matching and analytic extension, *J. Fluid. Mech.*, 85, 769–786, 1978.
- Ostrovsky, L. A., Hare, J. E., Smirnov, A., Kropfli, R. A., Naugolnykh, K., Skirta, E., and Stanton, T. P., in: *The action of swell and internal waves on short surface waves: in situ and radar observations*, (Ed) Banner, M. L., *Proceedings of the Symposium on the Wind-Driven Air-Sea Interface*, Sydney, Australia, 391–398, 1999.
- Phillips, O. M.: *The dynamics of upper ocean*, Cambridge University Press, 1977.
- Plant, W. J., Dahl, P. H., and Keller, W. C.: Microwave and acoustic scattering from parasitic capillary waves, *J. Geophys. Res.*, 104, 25 853–25 866, 1999.
- Ruvinskii, K. D. and Freidman, G. I.: The generation of capillary-gravity waves by steep gravity waves, *Izvestia, Atmos. and Ocean. Phys.*, 17, 548–553, 1981.
- Ruvinskii, K. D., Feldsteyn, F. I., and Freidman, G. I.: Effect of the nonlinear damping, associated with the generation of capillary-gravity ripples, on the stability of short wind waves and their modulation by a train of internal waves, *Izvestia, Atmos. Ocean. Phys.*, 22, 219–224, 1986.
- Smith, J.: Short surface waves with growth and dissipation, *J. Geophys. Res.*, 91, 2616–2632, 1986.
- Zhang, J. and Melville, W. K.: Evolution of weakly nonlinear short waves riding on long gravity waves, *J. Fluid. Mech.*, 214, 321–346, 1990.